PACS 42.25.Bs, 42.65.-K

Influence of two-photon absorption on polarization of light traveling in uniaxial crystals

M.R. Kulish, M.P. Lisitsa, N.I. Malysh
V. Lashkaryov Institute of Semiconductor Physics, NAS of Ukraine
41, prospect Nauky, 03028 Kyiv, Ukraine
E-mail: n_kulish@yahoo.com

Abstract. Investigated in this work is the influence of two-photon absorption on the major semiaxis angle rotation, ellipticity, focal parameter and eccentricity of polarization ellipse of light traveling in uniaxial single crystals. Influence of pumping intensity, angle of phase lag, coefficients of one-photon and two-photon absorption on polarization of light propagating in CdS single crystal is studied. Lasers, with the steady-state temperature of active body, which generate the pulse nanosecond duration and 0.1 pm line width radiation or lasers that generate the pulse with duration less than 300 fs are necessary to be used. The criteria to choose semiconductor parameters for providing optimum conditions for researches of light polarization at presence of two-photon absorption are formulated.

Keywords: CdS, two-photon absorption, ellipticity, ellipse of polarization.

Manuscript received 06.03.09; accepted for publication 18.03.09; published online 20.03.09.

1. Introduction

Different speed of traveling of ordinary and extraordinary light beam in uniaxial crystal and different value of extinction of their intensity is responsible for transformation of linear light polarization to the elliptic one. When linear optics laws (low intensity) are valid, the first mechanism prevails in the crystal transmission band ($h\nu < E_g$, where $h\nu$ is the light quantum energy, E_g is the forbidden gap), and second – in the absorption edge region. Changes in the shape of polarization ellipse, which take place here, are explored carefully [1].

In the case of nonlinear optics laws (high intensity), decrease in the intensity of light traveling in transparent crystal takes place as a result of multiphoton absorption. Two-photon absorption a most strongly influences on the light intensity. It dominates in the spectral range $E_g/2 < h\nu < E_g$. In uniaxial crystals, the coefficients of two-photon absorption for the electromagnetic wave parallel and perpendicular to the optical axis are different [2-4]. Hence, two-photon absorption must influence on light polarization pattern [5-7]. However, changes in the shape of the polarization ellipse, which take place here, remain unstudied. In this paper, we found equations that describe influence on two-photon absorption on the major semiaxis angle rotation, factor of compression, eccentricity and focal parameter of polarization ellipse. It is shown that in CdS computed dependences of these parameters versus azimuth of polarization quantitatively agree with those measured experimentally. The criteria to choose semiconductor parameters and laser are formulated to be used in researches of the influence of two-photon absorption on light polarization.

2. Samples and method of measurements

Plane parallel uniaxial single crystals of CdS 5 mm in thickness were used. Light beam falls at right angle to entrance surface of these crystals (Fig. 1). The optical axis in these crystals is parallel to entrance surface and to the axis OY (Fig. 1, insertion *a*). Single crystal CdS is placed between polarizer and analyzer. The fixed value of the angle φ (polarization azimuth) between the optical axis and vector **E** is related by crystal rotation. A thermally-stabilized (stability of temperature in laser active body is kept at the level ±0.07°) ruby laser with 20 ns pulse duration and with 1 pm half-width was used as a light source. The photomultipliers ELU-FT served as light detectors. Intensity of light on the entrance and output of the sample was determined with the error less than 10 %. Variation of the intensity was fulfilled by rearrangements of neutrally-grey filters from the set located before the sample into that located after the sample.

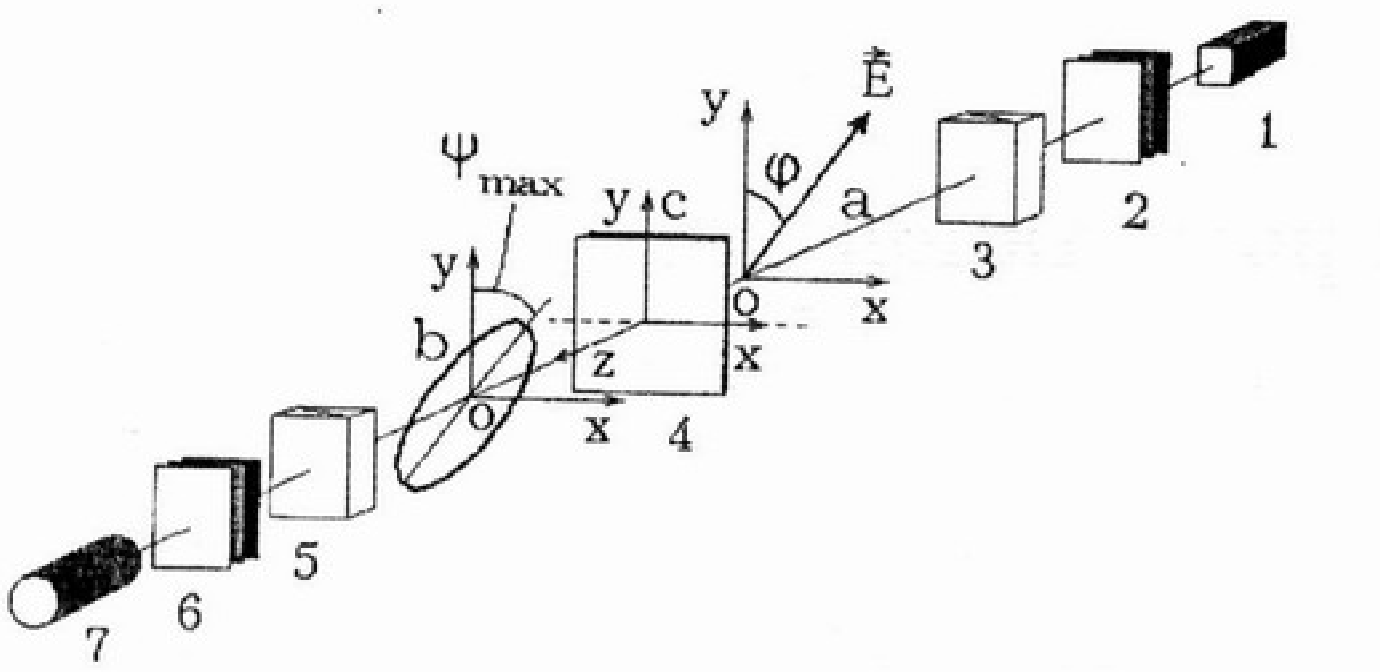

Fig. 1. Experimental setup used to research the influence of two-photon absorption on light polarization: ruby laser (*1*); sets of calibrated neutrally-grey filters (*2* and *6*); polarizer (*3*) (Glan prism); single crystal CdS, optical axis of which is parallel to the axis *y* (*4*); analyzer (*5*) (Glan prism); photomultiplier ELU-FT (*7*). Shown in the insertion *a* is orientation of the polarization vector of electromagnetic wave **E** with regard to the optical axis *C* on the entrance surface of uniaxial crystal, φ is the polarization azimuth. Shown in the insertion *b* is the shape of polarization ellipse on the output surface of the crystal, ψ_{max} is the angle on which the major semiaxis of polarization ellipse will be turned with regard to the optical axis *C* after transmission of light through the crystal.

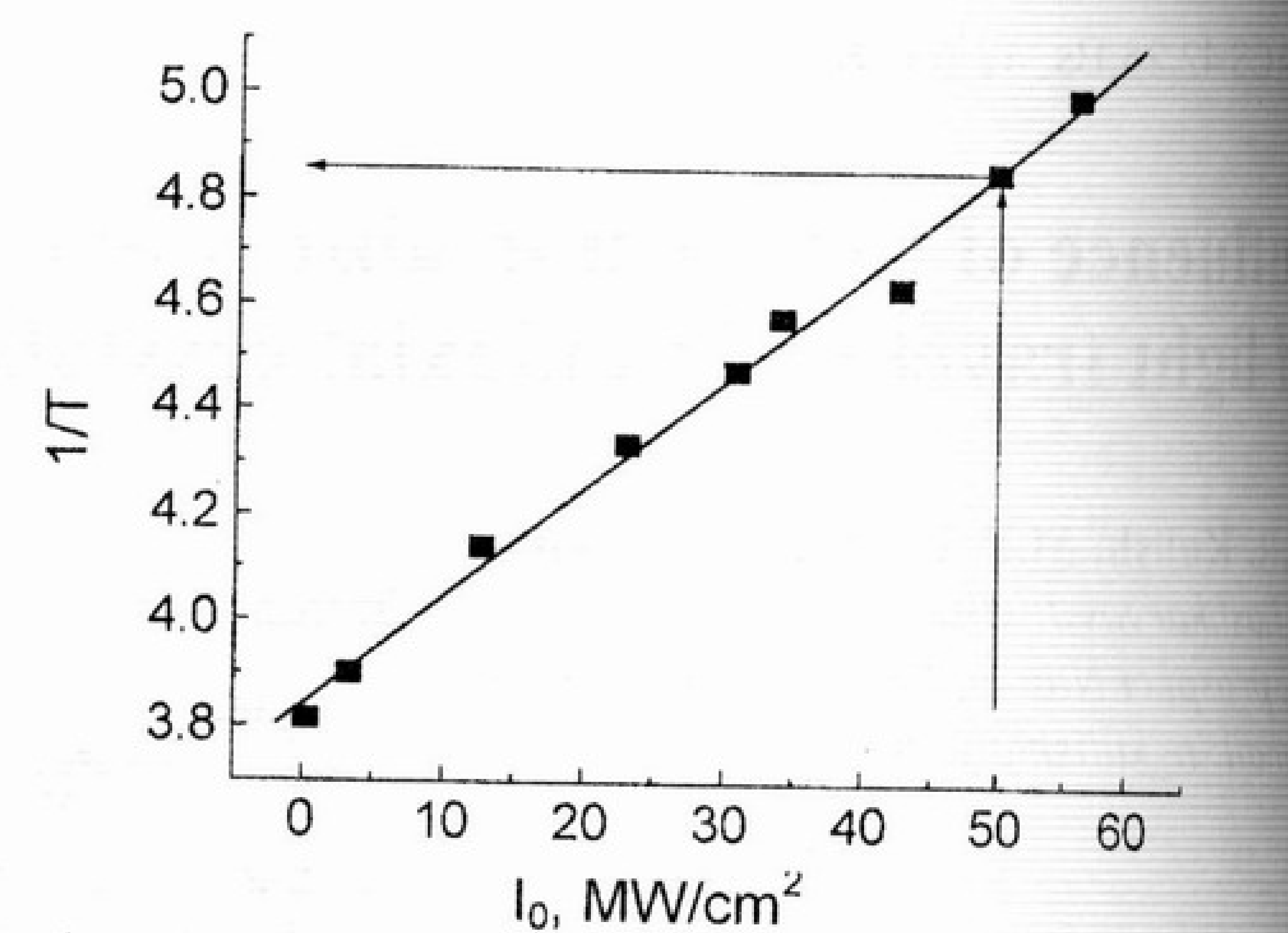

Fig. 2. Dependence of the reverse transmission $1/T$ versus intensity I_0 of linearly polarized light, which falls at the right angle to entrance surface of the crystal CdS of 5 mm thickness. The azimuth of polarization $\varphi = -15°$, ψ_{max} is the angle between the orientation of the polarization vector of electromagnetic wave after the analyzer and optical axis *C*. Points indicate the experimental data, solid line is calculation using the formula (1). $\psi_{max} = -60°$. Arrows show the method of determination of the intensity at the output of the sample.

In the case of two-photon absorption, the reverse transmission $1/T$ of the sample linearly depends on I_0 [2, 4]:

$$\frac{1}{T} = \frac{I_0}{I} = \frac{\exp(Kd)}{(1-R)^2} + \frac{\beta[\exp(Kd)-1]}{K(1-R)} I_0 = A + BI_0, \quad (1)$$

where K and β are coefficients for one-photon and two-photon absorption, d and R are the thickness and reflection coefficient of the sample, A and B are constants. Using the experimentally determined series values I and I_0, we plot a graph dependence $1/T = f(I_0)$ (Fig. 2, points). Every point in it was averaged over 20-30 measurements. The empiric dependence of $1/T$ on I_0 is approximated by a straight line by using the least-squares method. The point of crossing this line with ordinate axis gives the value of the constant A, and the slope of line gives the value of the constant B. Inserting A and B into formulae

$$K = \frac{1}{d} \ln[A(1-R)^2], \quad (2a)$$

$$\beta = \frac{BK(1-R)}{A(1-R)^2 - 1}, \quad (2b)$$

we estimated K value ($K = 1.8$ cm^{-1}) and β. The error of estimation for K is ±10 % and β equals ±20 %. Fixing the polarization azimuth φ for a set of ψ values, we evaluated the dependence of $1/T = f(I_0)$ and from it the value I, which corresponds to a certain fixed value I_0 (Fig. 2). Estimating the values I and ψ in that way, we plot the graph dependence $I = f(\psi)$ (Fig. 3a, points).

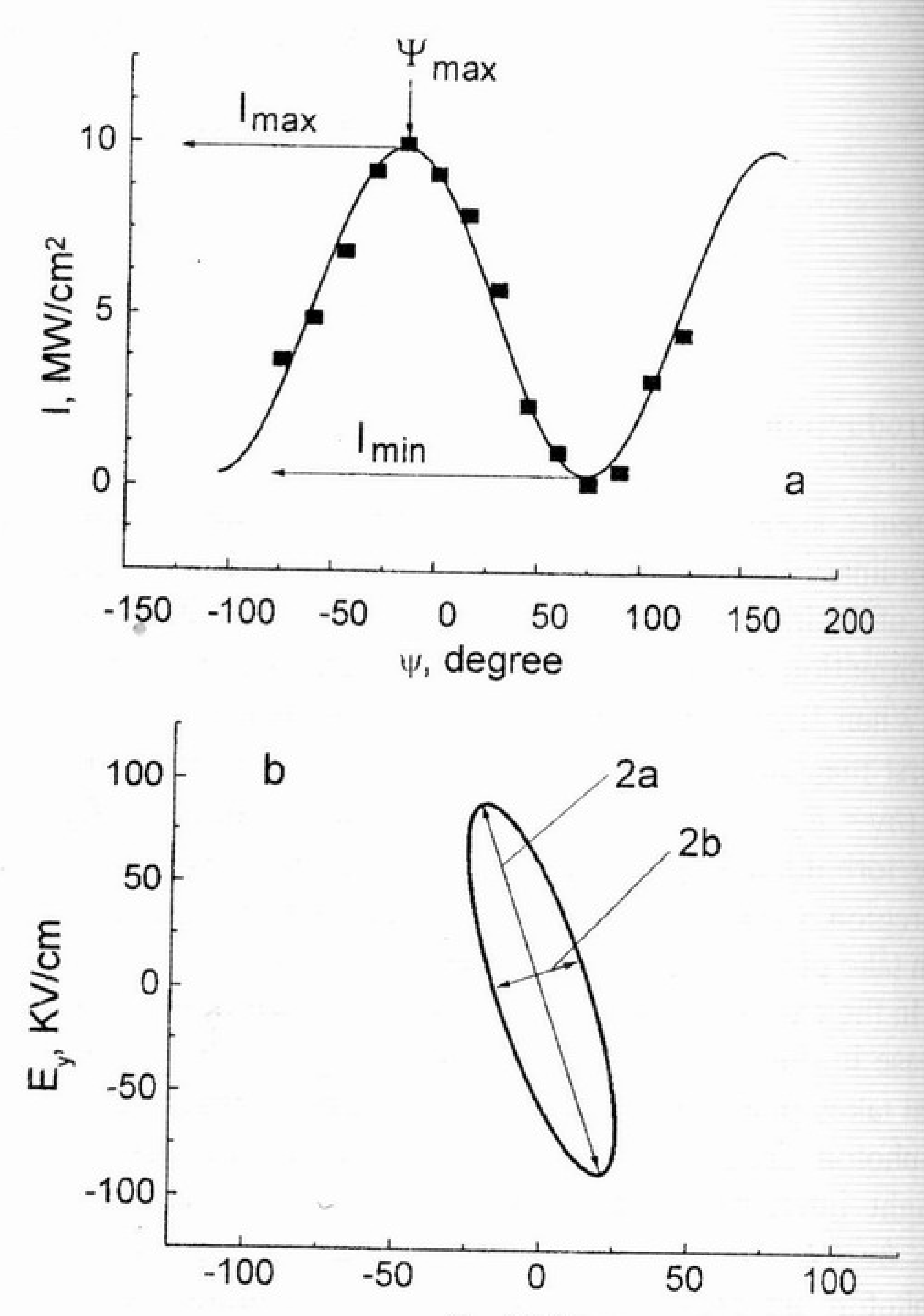

Fig. 3. Dependence of light intensity *I* that goes out of CdS crystal versus the rotation angle of the analyzer ψ (a) and shape of the polarization ellipse (b). Points indicate the experimental data, solid line is calculated using the formula (5). The azimuth of polarization $\varphi = -15°$, $I_0 = 50$ MW/cm^2. 2a and 2b are the lengths of major and minor axes of the polarization ellipse, respectively.

3. Influence of two-photon absorption on light polarization

Let the monochromatic linearly polarized light beam falls at the right angle to entrance surface of a uniaxial crystal (Fig. 1). It is possible to consider that two components of light beam travel in one-way in this crystal, if the azimuth $\varphi \neq n\pi/2$ ($n = 0, 1, 2, 3, \ldots$). $\mathbf{E} \perp C$ is one of the components, and $\mathbf{E} \| C$ – another. Directly behind the crystal entrance surface, the intensities of these components are as follows:

$$I_{0\perp} = I_0 \cos^2\varphi, \tag{3a}$$
$$I_{0\|} = I_0 \sin^2\varphi. \tag{3b}$$

If light propagates in a crystal transmission band, the intensity of these light decreases as a result of two-photon absorption and outside the crystal these intensities are equal:

$$I_\perp = \frac{I_0(1-R_\perp)^2 \cos^2\varphi\, e^{-K_\perp d}}{1 + \frac{\beta_\perp I_0 (1-R_\perp)\cos^2\varphi}{K_\perp}\left(1 - e^{-K_\perp d}\right)} = \frac{I_0(1-R_\perp)^2 \cos^2\varphi\, e^{-K_\perp d}}{1 + D_\perp}, \tag{4}$$

$$I_\| = \frac{I_0(1-R_\|)^2 \sin^2\varphi\, e^{-K_\| d}}{1 + \frac{\beta_\| I_0 (1-R_\|)\sin^2\varphi}{K_\|}\left(1 - e^{-K_\| d}\right)} = \frac{I_0(1-R_\|)^2 \sin^2\varphi\, e^{-K_\| d}}{1 + D_\|}. \tag{5}$$

At the analyzer output, the light intensity is as follows:

$$I = I_\perp \cos^2\psi + I_\| \sin^2\psi + \sqrt{I_\perp I_\|}\sin(2\psi)\cos\delta, \tag{6}$$

where δ is the angle phase lag. The values $I_\perp$ and $I_{||}$ are estimated using the formulae (4) and (5).

Influence of two-photon absorption on polarization of light that travels in CdS was studied at $I_0 =$ 50 MW/cm^2 and several polarization azimuths. For all the φ values, the dependence $I = f(\psi)$ looks like that presented in Fig. 3a. The dependence (solid line) calculated using the formula (6) is in agreement with the experimental dependence (points), if using the right choice of the value δ. At the optimum value $\delta = -40°$, the error of approximation is less than 5 %. The values of minimum ($I = I_{min}$) and maximal ($I = I_{max}$) intensities, and the value of the angle ($\psi = \psi_{max}$) providing the equality $I = I_{max}$, we can easily find using the data of Fig. 3. Then, applying the known correlation between the intensity I and electric field E [8]

$$E[\text{V/cm}] = 27.46 \cdot I^{0.5}\,[\text{W/cm}^2], \tag{7}$$

we find the shape of polarization ellipse (Fig. 3b).

Every ellipse we can characterize by the angular position of its major semiaxis in relation to Carthesian coordinates, compression factor, eccentricity and focal parameter. Values of these parameters depend on the coefficient of two-photon absorption.

Position of the major semiaxis ψ_{max} depends on the azimuth of polarization φ, thus

$$\tan(2\psi_{max}) = \frac{2I_\perp^{0.5} I_\|^{0.5}}{I_\| - I_\perp}\cos\delta. \tag{8}$$

In the course of approximation of the empiric dependence $\psi_{max} = f(\varphi)$, the values $R_\perp = R_{||} = 0.2$, $I_0 =$ 50 MW/cm^2 were inserted in the formula (8). Also inserted in the formula (8) were the values $K_\perp$, $K_{||}$, $\beta_\perp$, $\beta_{||}$, found as a result of processing the dependences $1/T = f(I_o)$ that were measured at $\varphi = 0°$ and $\varphi = 90°$. It is shown that the calculated (Fig. 4a, solid line) and empiric (Fig. 4a, points) dependences numerically agree with each other.

Deviation ellipse ratio from a circle is the compression factor or ellipticity

$$\chi = \frac{b}{a}\sqrt{\frac{I_{min}}{I_{max}}}, \tag{9}$$

where b and a are the lengths of minor and major semiaxes of the polarization ellipse (Fig. 3b), I_{min} and I_{max} are minimum and maximal values of the intensity at the analyzer output (Fig. 3a). The intensities I_{min} and I_{max} were estimated by the formula (6), in which the known values of $K_\perp$, $K_{||}$, $\beta_\perp$, $\beta_{||}$ were inserted. The value of the angle ψ_{max} was estimated using the formula (8) and was also inserted in the formula (6).

In full accordance with the formula (9) at $\varphi = 0°$ and $\varphi = 90°$, the ellipse degenerates in a straight line. The maximal proximity to the circle is achieved at $\varphi = -45°$ (Fig. 4b).

The eccentricity of the ellipse is as follows:

$$\xi = \frac{\sqrt{a^2 - b^2}}{a} = \sqrt{\frac{I_{max} - I_{min}}{I_{max}}}. \tag{10}$$

In accordance with the data of Fig. 4c, there is a quantitative correspondence between the empiric dependence ξ on φ and that calculated using the formula (10). The minimum value ξ is realized when $\varphi = -45°$.

The focal parameter

$$p = \frac{b^2}{a} = \frac{27.46\, I_{min}}{2\sqrt{I_{max}}} \tag{11}$$

characterizes the change of the polarization ellipse in points crossing the perimeter by the chord that run out through focus and is parallel to the minor axis. The dependence p on φ calculated by the formula (11) and empiric data are given in Fig. 4d.

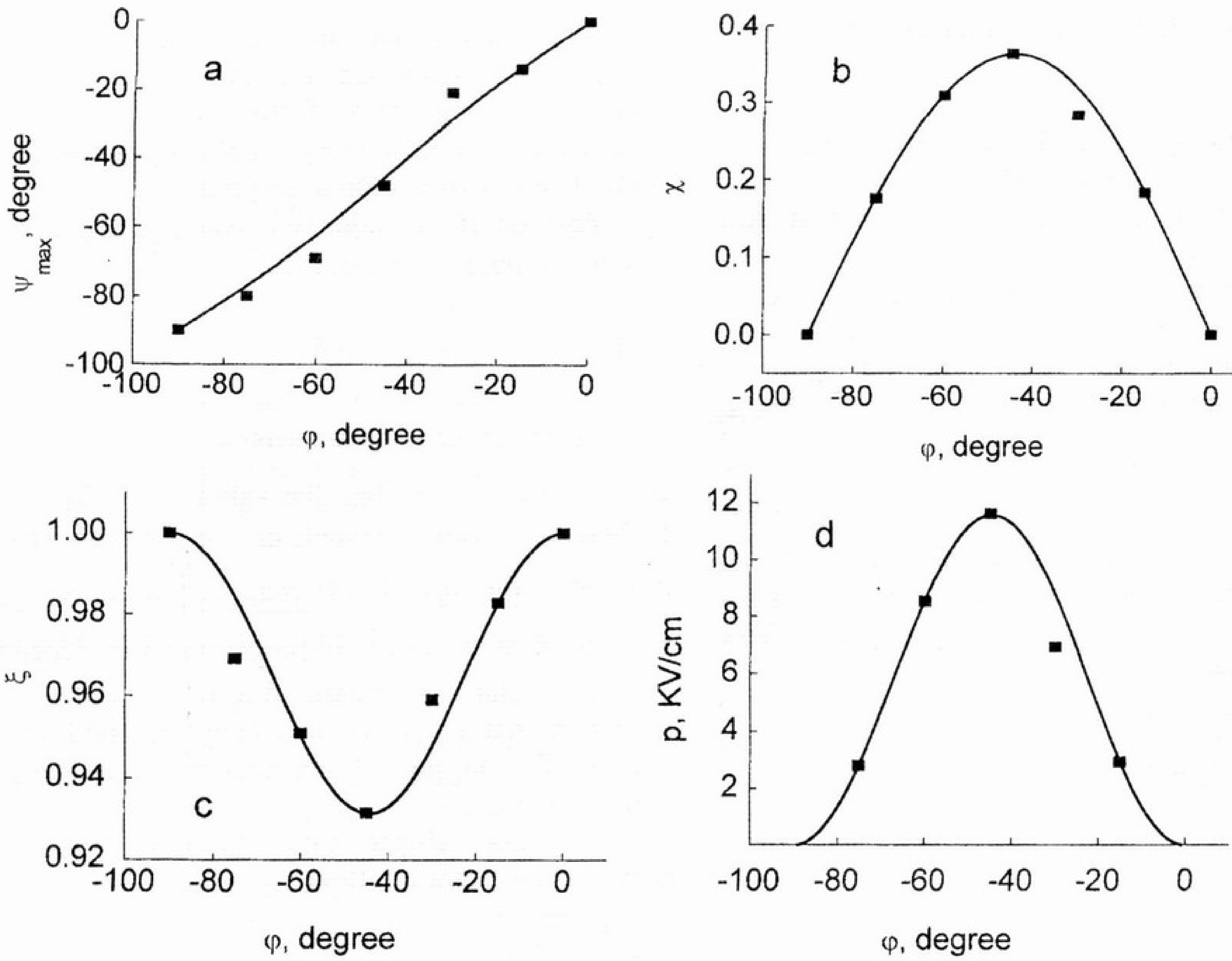

Fig. 4. Dependences of the angle ψ_{max} for rotation of the major semiaxis of polarization ellipse relatively to the optical axis C (*a*), ellipticity χ (*b*), eccentricity ξ (*c*) and focal parameter p (*d*) on the polarization azimuth φ. The pumping intensity I_0 = 50 MW/cm², λ = 694.3 nm. Solid curves were calculated using the formulae: *a* – (8), *b* – (9), *c* – (10), *d* – (11).

The quantitative matching of experimental dependences ψ_{max}, χ, ξ, p on φ with the calculated ones allows to use the formulae (4)-(6) for determination of conditions that provide the influence of two-photon absorption on the shape of the polarization ellipse to be maximal. The purpose of this analysis consists in studying the features of the influence of crystal parameters and light source on the polarization pattern and determination of the conditions, under fulfillment of which two-photon absorption has a strong influence on the polarization pattern. These considerations will be done using CdS as an example.

4. Optimization polarization pattern of light by the angle of phase lag

In accordance with the formula (6), when δ increases gradually from 0° to 90°, the light intensity I at the output of the sample is gradually decreased from $I = \left(\sqrt{I_\perp}\sin\psi + \sqrt{I_\parallel}\cos\psi\right)^2$ to $I = I_\perp \sin^2\psi + I_\parallel \cos^2\psi$. Change of parameters of the polarization ellipse observed in this case is shown in Fig. 5. When $\delta = 0°$, there is a linear dependence of ψ_{max} on φ (Fig. 5a, curve 1). This dependence is modulated by $\cos\delta$. The modulation depth grows with the increase of δ. When the value $\delta = 90°$, there occurs a stepwise change of the dependence of ψ_{max} on φ (Fig. 5a, curve 5). This jump takes place at $\varphi = -45°$. At this value of the azimuth, the sine-like dependence of the numerator in the formula (8) becomes like to cosine. At the same time, for all the values of δ at increasing φ there is a gradual increase in the ellipticity (Fig. 5b) and focal parameter (Fig. 5d) as well as decrease in the eccentricity (Fig. 5c). The maximal changes of these parameters take place at $\varphi = -45°$. With the following increase of the polarization azimuth, χ and a phase p reveal lag within the range $40° < \delta < 90°$. In what follows, we will name this range as the actual one.

It is known [1] that the value of the phase lag angle

$$\delta = \frac{2\pi d\left(n_o - n_e\right)}{\lambda} \qquad (12)$$

depends on the difference ($\Delta n = n_o - n_e$) of refraction indexes for the ordinary (n_o) and extraordinary (n_e) beams, excitation wavelength (λ) and thickness of the crystal (d). Changing any of these parameters is possible to change the value δ and $\cos\delta$, and hence, the light intensity (see the formula (6)).

Wavelength. The character of dependences for δ and $\cos\delta$ versus λ is shown in Fig. 6a. One can see that, in the vicinity of λ = 694.3 nm, the actual region of δ changes ($40° < \delta < 90°$) suit the spectral range $\Delta\lambda$ =

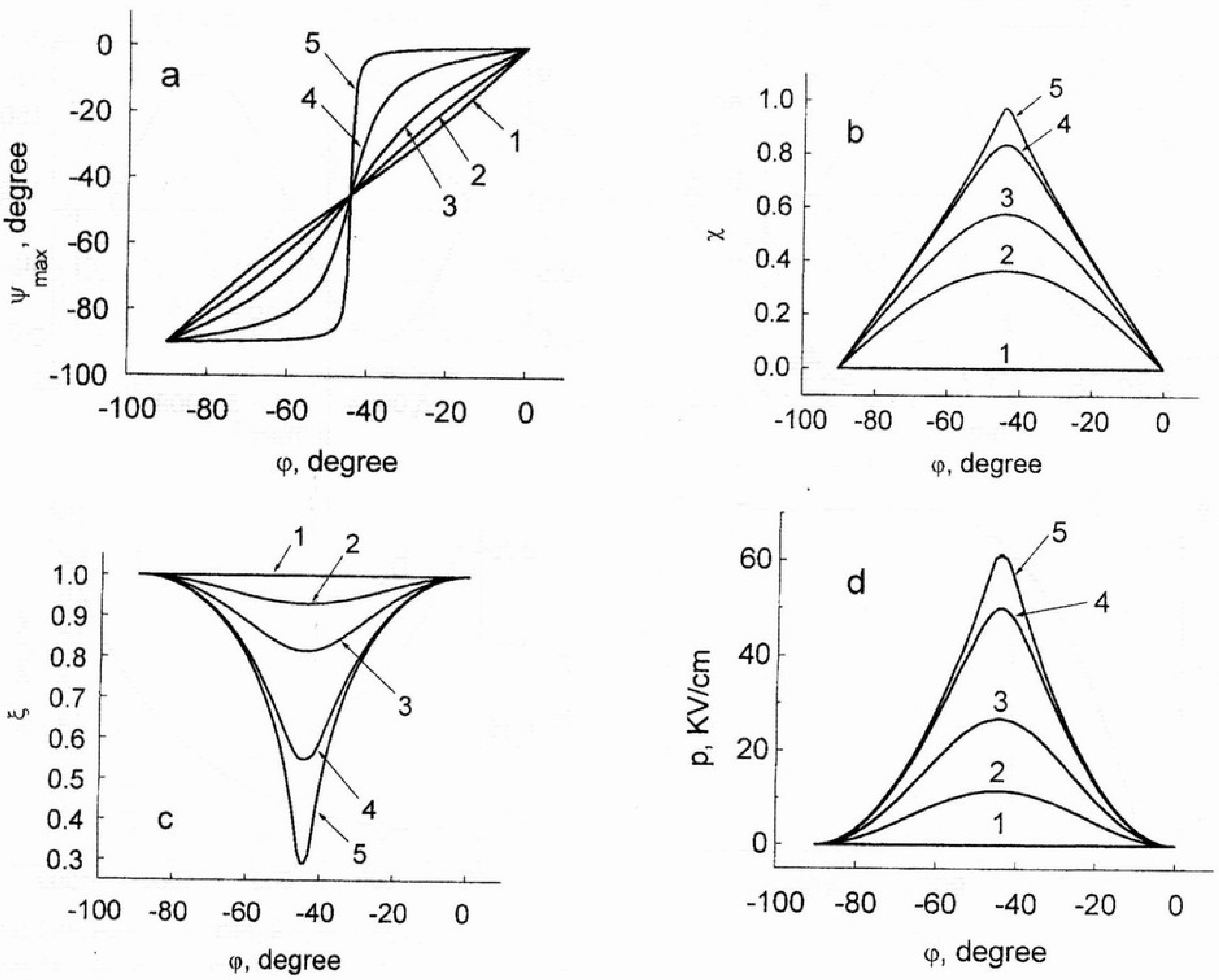

Fig. 5. Dependences of the phase lag angle and polarization ellipse parameters: the angle of rotation of ellipse major semiaxis (*a*), compression factor (*b*), eccentricity (*c*), focal parameter (*d*) on the polarization azimuth φ. The value of the phase lag angle in degrees: *1* – 0; *2* – 40; *3* – 60; *4* – 80; *5* – 89.

6.7 pm (Fig. 6b). The dimension of this spectral range depends on the excitation light wavelength. Near the $\lambda = 520$ nm, it equals $\Delta\lambda = 0.13$ pm. It means that the study of the influence of the phase lag angle on light polarization requires sources with the half-width of the radiation line less than one tenth of this range. They are lasers that can serve as these sources. In particular, the half-width $\Delta\lambda_g$ of the generation line in our ruby laser is equal to 1 pm. Its relationship with the length of a spectral range is shown in Fig. 6a. A single-mode ruby laser generates a line with the half-width $\Delta\lambda_g < 0.1$ pm [10]. Dye lasers with a grating dispersion element in their resonators generate lines with the half-width $\Delta\lambda_g = 50$ pm [11]. $\Delta\lambda_g$ decreases to 1 pm, when in the resonator of such laser one mounts a standard Fabry-Perot element [11].

Thickness of crystal. The dependences of δ and cosδ on the crystal thickness *d* are shown in Fig. 7a. For light with $\lambda = 694.3$ nm, the actual region of δ changes ($40° < \delta < 0°$) corresponds to the interval of crystal thickness variation $\Delta d = 100$ nm. It means that to vary δ by its value within the above range, it is necessary to change *d* with a step of the order of 10 nm. Technically, to realize the change in the crystal thickness with such an exactness (even by etching or epitaxy) is very difficult and inconvenient, since non-parallelism of crystal surfaces should be kept at the level 1 nm. Transition to longer waves is accompanied by the increase in Δd (Fig. 7b), but this does not save the situation.

Difference of refraction indexes. For majority of uniaxial crystals, the dependence of n_o and n_e on λ is known and tabulated [9, 12], and consequently the dispersion Δn is known. In CdS for $\lambda = 694.3$ nm, the actual region of δ changes ($40° < \delta < 90°$) meet the interval of variations in the value $\Delta n = (n_o - n_e) = 3.35 \cdot 10^{-7}$. It means that, when studying the influence of δ on parameters of the polarization ellipse, it is necessary to give advantage to the crystals that have no dependence of Δn on the external factors.

Influence of temperature. Such semiconductor parameters as n_o, n_e and *d* determine the value δ, but they depend on temperature. It has been experimentally shown in [13] that n_o and n_e linearly increases with temperature, namely:

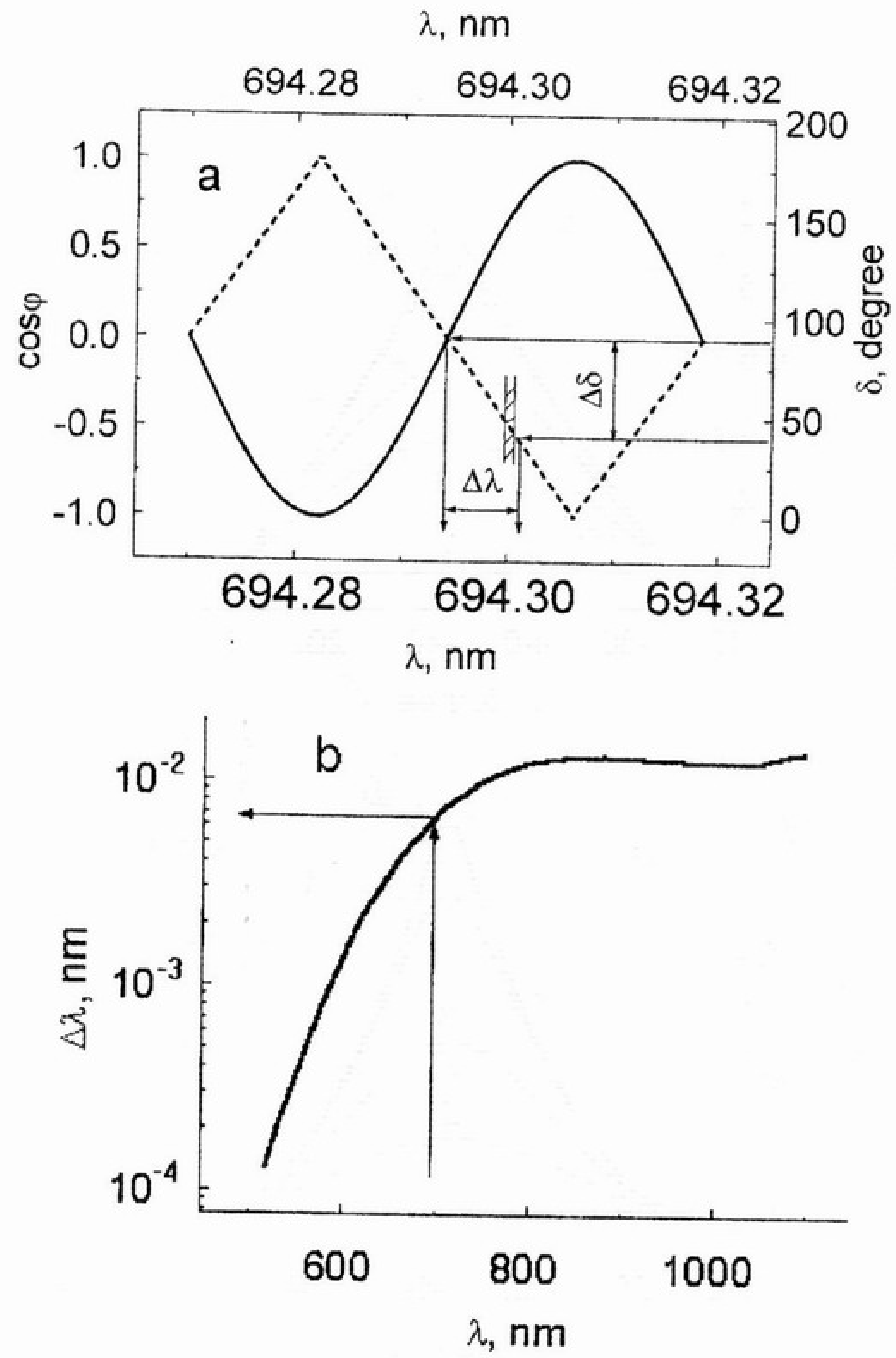

Fig. 6. (a) Wavelength dependence of the phase lag angle (δ) (dotted curve) and cosδ (solid curve), as well as (b) width of spectral region in which substantial changes of parameters of the polarization ellipse take place. Δδ and Δλ are the regions where the polarization ellipse parameters substantially depend on the phase lag angle (δ) and on the wavelength. The shaded area meets the half-width of line of ruby laser generation. Spectral position of this line in Fig. 6b is marked by the vertical line. The horizontal line indicates the value of the spectral range width.

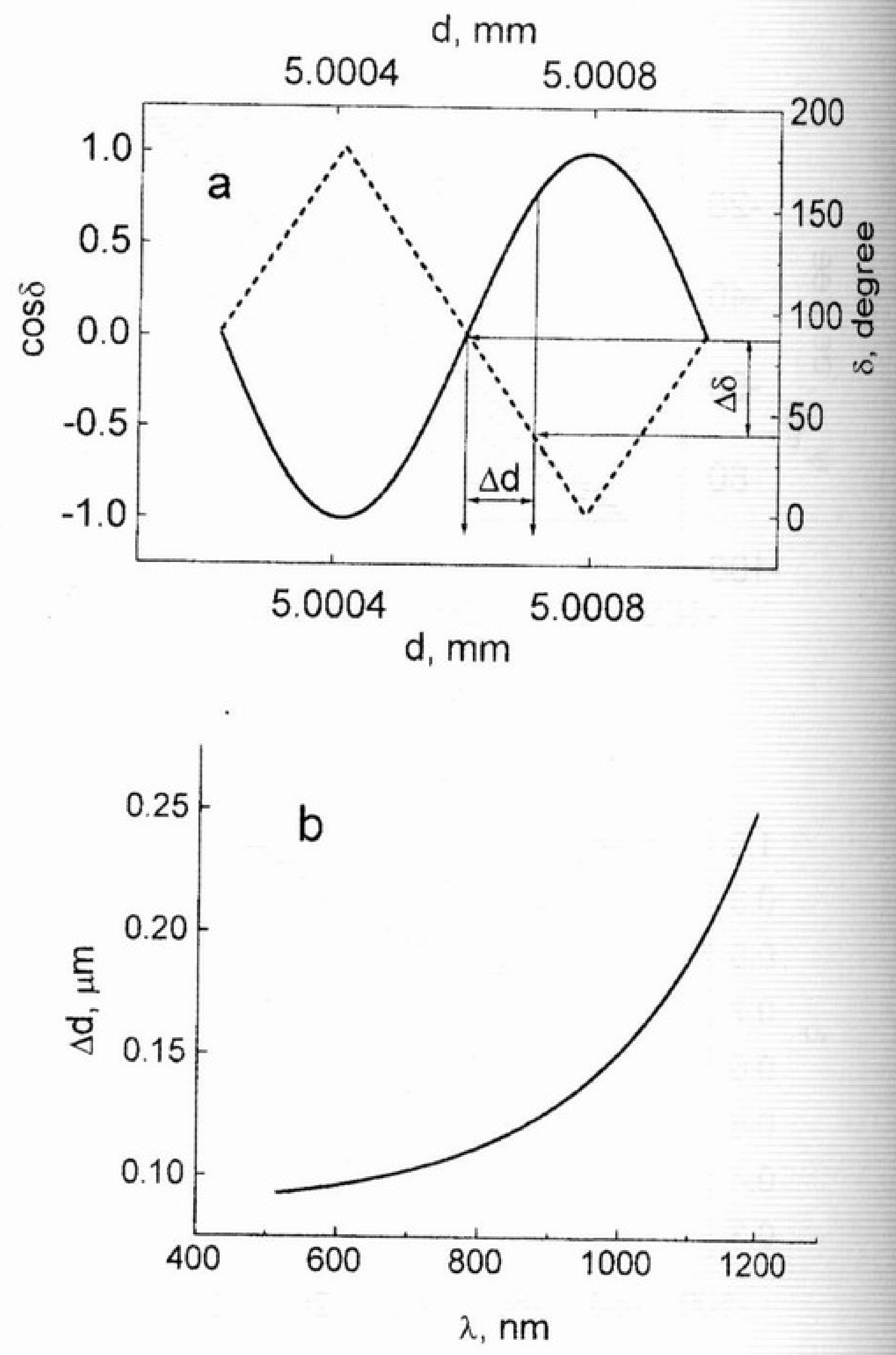

Fig. 7. (a) Sample thickness dependence of the phase lag angle δ (dotted curve) and cosδ (solid curve), as well as (b) the wavelength dependence of changes in the sample thickness within the region where we have a strong influence of the pumping wavelength on parameters of the polarization ellipse. Δδ and Δd are the regions in which parameters of the polarization ellipse substantially depend on the phase lag angle.

$$N_o(T) = n_o(T_o) + \Gamma_o (T - T_o), \tag{13}$$

$$n_e(T) = n_e(T_o) + \Gamma_e (T - T_o), \tag{14}$$

where T and T_o are the final and initial temperature (in Kelvins), Γ_o and Γ_e are that parameters the value of which depends on λ. In accordance with calculations [13], which are experimentally confirmed, the values of Γ_o and Γ_e do not depend on temperature. Authors of [13] have been shown that $\Gamma_o = \Gamma_e$. It means that Δn does not depend on temperature. The length of waves generated by lasers depends on temperature. In particular, within the range 20 °C < t < 80 °C (t is a temperature in Celsius degrees), the change in temperature of ruby rod by $\Delta t_u(°C) = \Delta\lambda_g(nm)/0.0068 = 0.07$ °C gives the change in the wavelength of ruby laser by 0.5 pm [14]. Temperature stability of ruby rod with this accuracy can be easily realized by the methods described in [15].

We use the property of solids to change their size under action of temperature to choose the required δ value. Relation between the thickness of the crystal d and temperature is as follows:

$$d = d_0 (1 + \gamma t), \tag{15}$$

where d_0 is the crystal thickness at $t = 0$ °C, γ is the coefficient of linear expansion. In CdS, for the direction parallel to the optical axis $\gamma = \gamma_{\parallel} = 3.5\cdot10^{-6}$ degree^{-1}, and for the direction perpendicular to the optical axis $\gamma = \gamma_{\perp} = 5.0\cdot10^{-6}$ degree^{-1} [11].

Taking into account the dependences of Δn, λ and d on temperature, we find the dependences of δ and cosδ on t (Fig. 8a). It is seen from the figure that, for λ = 694.3 nm, the actual range of temperature is equal to 4 °C. The dependence of this range from the wavelength is shown in Fig. 8b. With increasing λ, the size of this

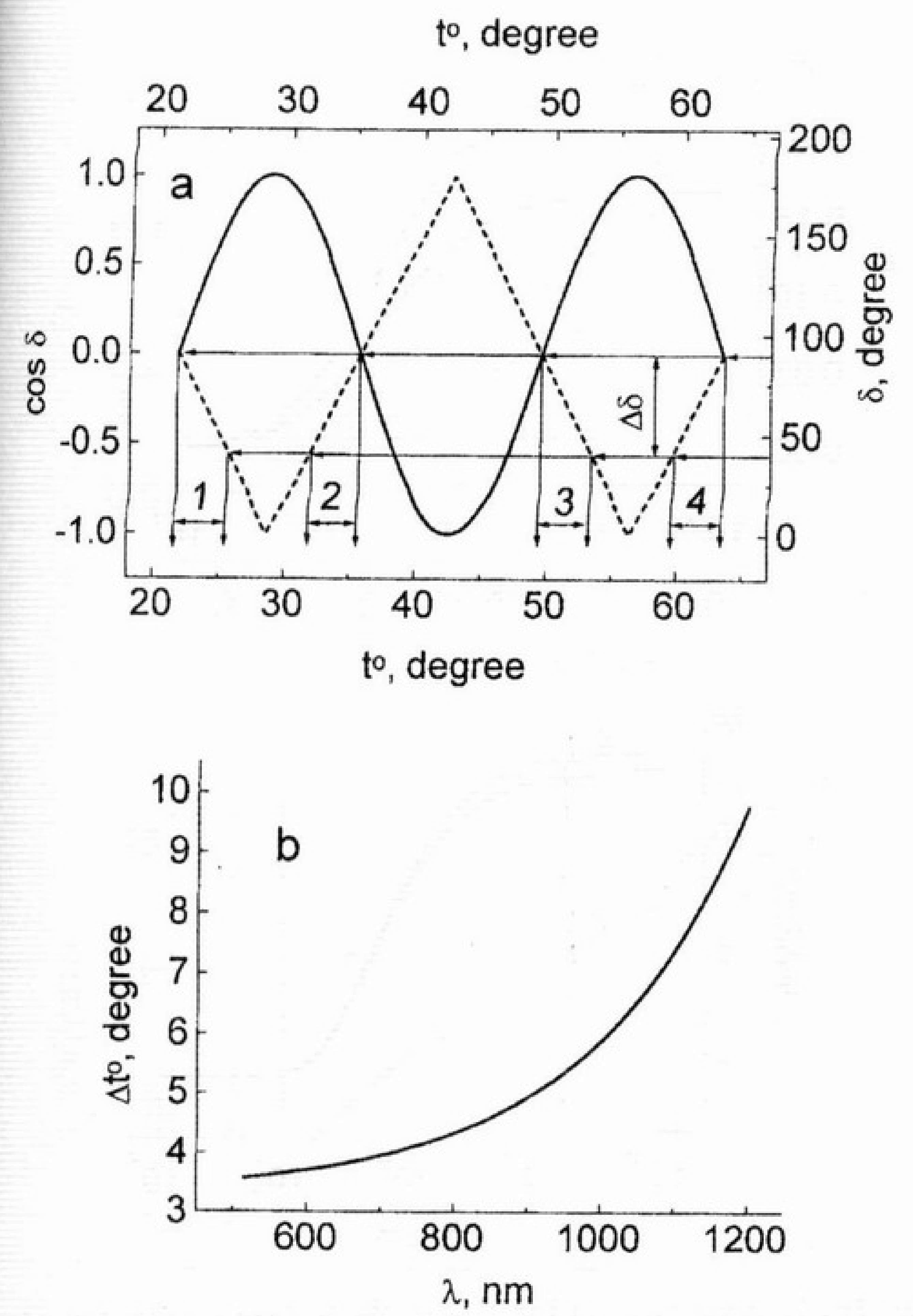

Fig. 8. (a) Influence of the sample temperature t on the angle δ of phase lag (dotted curve) and $\cos\delta$ (solid curve), as well as (b) influence of the wavelength on the range of temperature Δt, within the limits of which it is possible to vary the δ value. $\Delta\delta$ and t are the regions in which parameters of the polarization ellipse substantially depend on the phase lag angle. By arabic numerals we designate the positions of ranges within the limits of which it is possible to control the change of temperature.

range increases from 3.5 °C (for λ = 515 nm) to 13.5 °C (for λ = 1050 nm). The standard temperature controller [16] has an analog output signal which is proportional to temperature. The use of it allows to keep temperature in a thermostat with the error less than ±0.05 °C within the temperature range sufficient for purposeful change of the phase lag angle.

5. Optimization of conditions for studying the influence of the intensity of light traveling inside uniaxial crystal on polarization pattern

It is necessary to take into account the influence of the intensity of usual ($I_\perp$) and unusual ($I_{||}$) light beam on parameters of the polarization ellipse, when it is already impossible to ignore the second term (we will designate it accordingly through $D_\perp$ and $D_{||}$) in the denominator of equations (4), (5) in comparison with unity. The values $D_\perp$ and $D_{||}$ depend on the following parameters: $R_\perp$, $R_{||}$, d, $K_\perp$, $K_{||}$, I_0, $\beta_\perp$, $\beta_{||}$. Determination of the range within the limits of which it is possible to change one or *another parameter (at the fixed value of the other one)*, we will carry out for CdS. The value of parameter, when $D_\perp$ and $D_{||}$ differ from zero no more than 1 %, is taken as the lower limit, and for upper limit we take that value of parameter when it is already possible to ignore the changes in $I_\perp$ and $I_{||}$. In this analysis, we used the following values of parameters: $\delta = 40°$, I_0 = 50 MW/cm^2, $R = R_\perp = R_{||} = 0.2$, $K = K_\perp = K_{||} = 1.8$ cm^{-1}, $\beta_\perp$ = $2.4\cdot10^{-2}$ cm/MW, $\beta_{||}$ = $1.7\cdot10^{-2}$ cm/MW, d = 5 mm. These correspond to the parameters of CdS single crystal and ruby laser.

Coefficient of reflection. Changes of the reflection coefficient under the influence of temperature and atmospheric pressure fluctuations in the apartments of laboratories do not exceed 1 %. When analyzing the influence of light intensity on parameters of the polarization ellipse, we suppose that the coefficient of reflection is a constant, the value of which is inherent to specific semiconductor. To simplify the analysis, we assume that $R = R_\perp = R_{||}$.

Thickness of sample. The dependences of $D_\perp$, $D_{||}$, $I_\perp$, $I_{||}$ on d are shown in Fig. 9. One can see that second term of the denominator in equations (4), (5) differs from zero less than 1 % when $d < 0.3$ mm. It means that it is not necessary to use the samples with $d < 0.3$ mm for researches of polarization. If $d > 15$ mm, the values $D_\perp$, $D_{||}$ and $I_\perp$, $I_{||}$ do not practically depend on d. Therefore, the value $d = 15$ mm can be taken as the upper limit of the used crystal thickness. It should be noted that the difference between $I_\perp$ and $I_{||}$ is unimportant under any value of the crystal thickness (Fig. 9b). If δ is constant, it means that it is possible to ignore the influence of the crystal thickness on parameters of the polarization ellipse.

Single-photon absorption. If the coefficient of single-photon absorption K increases, a difference between $D_\perp$ and $D_{||}$ as well as that between $I_\perp$ and $I_{||}$ begins to diminish when K is less than 0.2 cm^{-1} (Fig. 10a). Consequently, when studying the influence of two-photon absorption on light polarization, it is preferably to use the samples with $K < 0.2$ cm^{-1}. The value $D = 0.01$ is achieved at $K = 50$ cm^{-1} (Fig. 10a). However, at $K \geq 10$ cm^{-1} the magnitudes of $I_\perp$ and $I_{||}$ do not depend on K (Fig. 10b). It means that the samples with $K \geq 10$ cm^{-1} are not necessary to be used when investigating the influence of two-photon absorption on light polarization.

Pumping intensity. An increase in the pumping intensity I_0 leads to growth of $D_\perp$, $D_{||}$ by a linear law (Fig. 11a), and to growth of $I_\perp$, $I_{||}$ by nonlinear law (Fig. 11b). If $I_0 < 4.5$ MW/cm^2, the second term of the denominator in equations (4), (5) differs from zero less than 1 % (Fig. 11a). It means that for polarization researches it is necessary to use the value

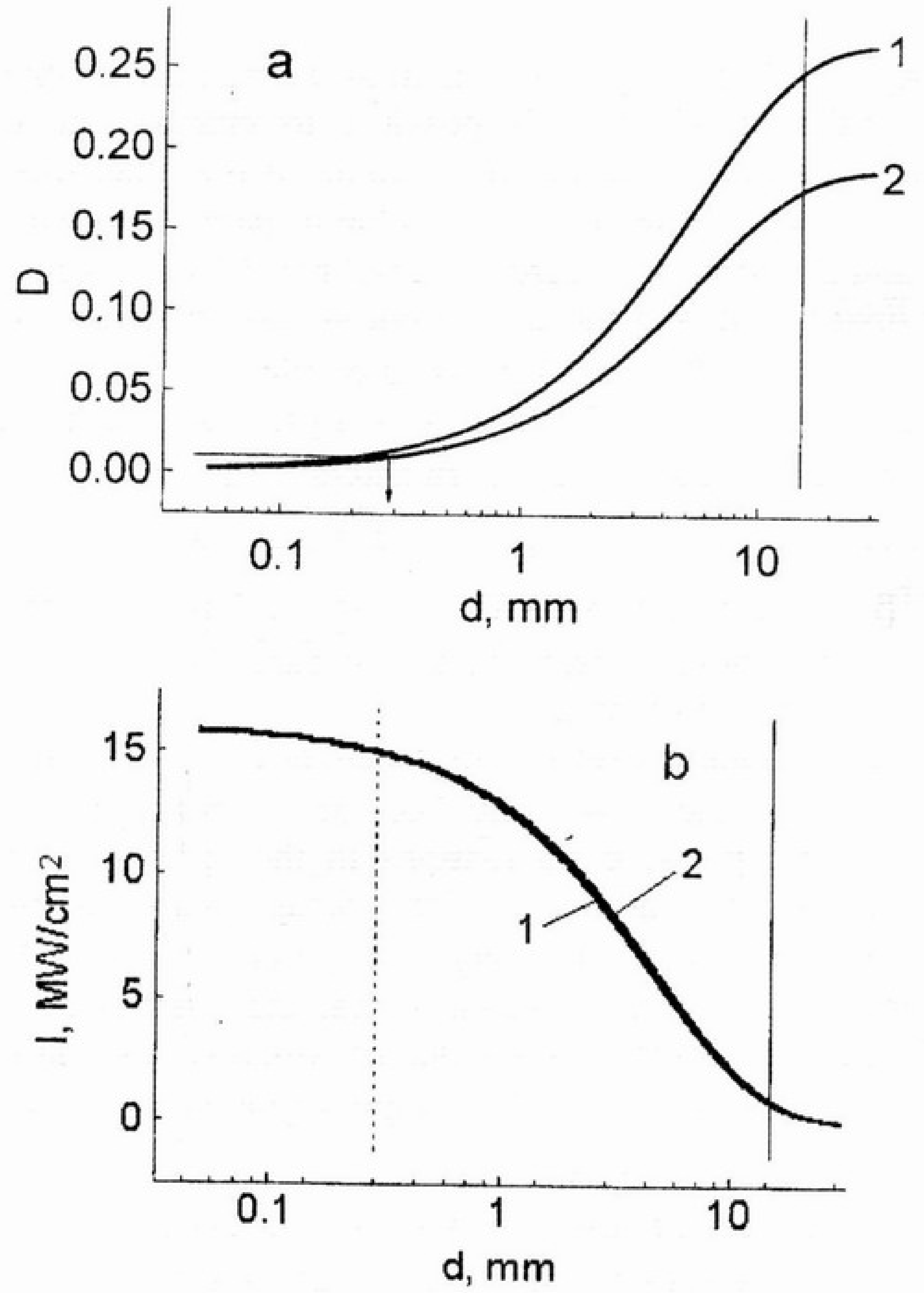

Fig. 9. Dependence on the crystal thickness d: a) second term ($D_{\perp}$, $D_{\parallel}$ in the denominator of formulae (4), (5); b) intensities of light beams ($I_{\perp}$, $I_{\parallel}$). Shown by the arrow is the crystal thickness, on achievement of which $D = 0.01$. The lower limit of single-crystal CdS thickness is shown by the dotted line, upper limit of thickness is shown by the solid line. *1* – $D_{\perp}$, $I_{\perp}$; *2* – $D_{\parallel}$, $I_{\parallel}$.

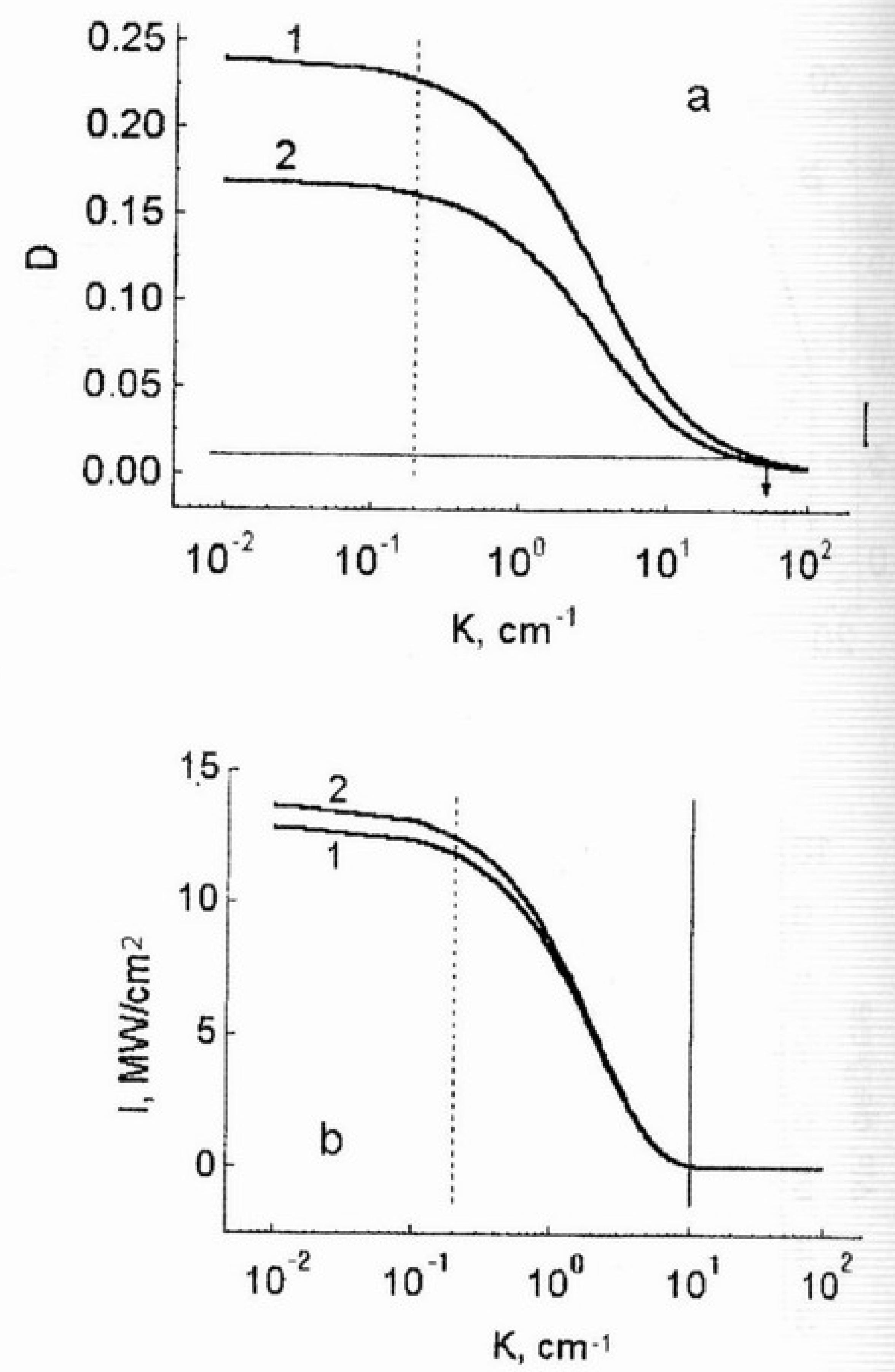

Fig. 10. Dependence on the linear absorption coefficient K: a) the second term ($D_{\perp}$, $D_{\parallel}$) in the denominator of the formulae (4), (5); b) intensities of light beams ($I_{\perp}$, $I_{\parallel}$). The linear absorption coefficient shown by arrow corresponds to $D = 0.01$. The lower limit of the range for changing the linear absorption coefficient is shown by the dotted line, the upper limit of thickness is shown by the solid line. *1* – $D_{\perp}$, $I_{\perp}$; *2* – $D_{\parallel}$, $I_{\parallel}$.

$I_0 > 4.5$ MW/cm^2. When $I_0 \geq 1100$ MW/cm^2, the values $D_{\perp}$, $D_{\parallel}$ are so high that we can to neglect by unity in the denominator of formulae (4), (5). In this case, the intensity components $I_{\perp}$ and $I_{\parallel}$ almost do not depend on I_0. It means that further growth of I_0 will not influence on polarization properties of light. However, at nanosecond duration of the pumping pulse, considerably before (in CdS at (110±10) MW/cm^2) the threshold I_t of optical erosion determines the upper boundary of changing I_0. Among all the possible mechanisms [17-19] (self-focusing, stimulated Brillouin scattering, stress of light, thermal heating of microparticless) causing optical erosion in transparent semiconductors the thermal one is basic [18]. Within the framework of this mechanism, the threshold of optical erosion can be estimated using the formula [18]

$$I_t = \frac{C^* \rho T_e}{K \tau}, \tag{16}$$

where K, ρ, C^* are the coefficients of one-photon absorption, specific density and specific heat of microparticles, respectively, τ is the duration of laser pulse, T_e is the temperature of evaporation for a non-transparent microparticle, which is accompanied by local microexplosion with the damage of semiconductor. As it is shown by the formula (18), the threshold I_t of optical erosion is possible to be increased by means of decreasing the laser pulse duration. So, I_t increases to 150 GW/cm^2, if we decrease τ to 3 ps [19]. However, diminishing τ is accompanied by increasing the linewidth of laser generation [20] as

$$\Delta\nu\Delta\tau = \frac{c\,\Delta\lambda_g}{\lambda^2}\tau = 1, \tag{17}$$

where $\Delta\lambda_g$, $\Delta\nu$ is the linewidth of laser generation in nanometers and in Hertzs, accordingly, c is the speed of light in vacuum. If $\Delta\lambda_g$ is commensurable with the region ($\Delta\lambda$) of the effective influence of wavelength on the phase lag angle (Fig. 6), it is necessary to average the third term by δ in the formula (6). In particular, at

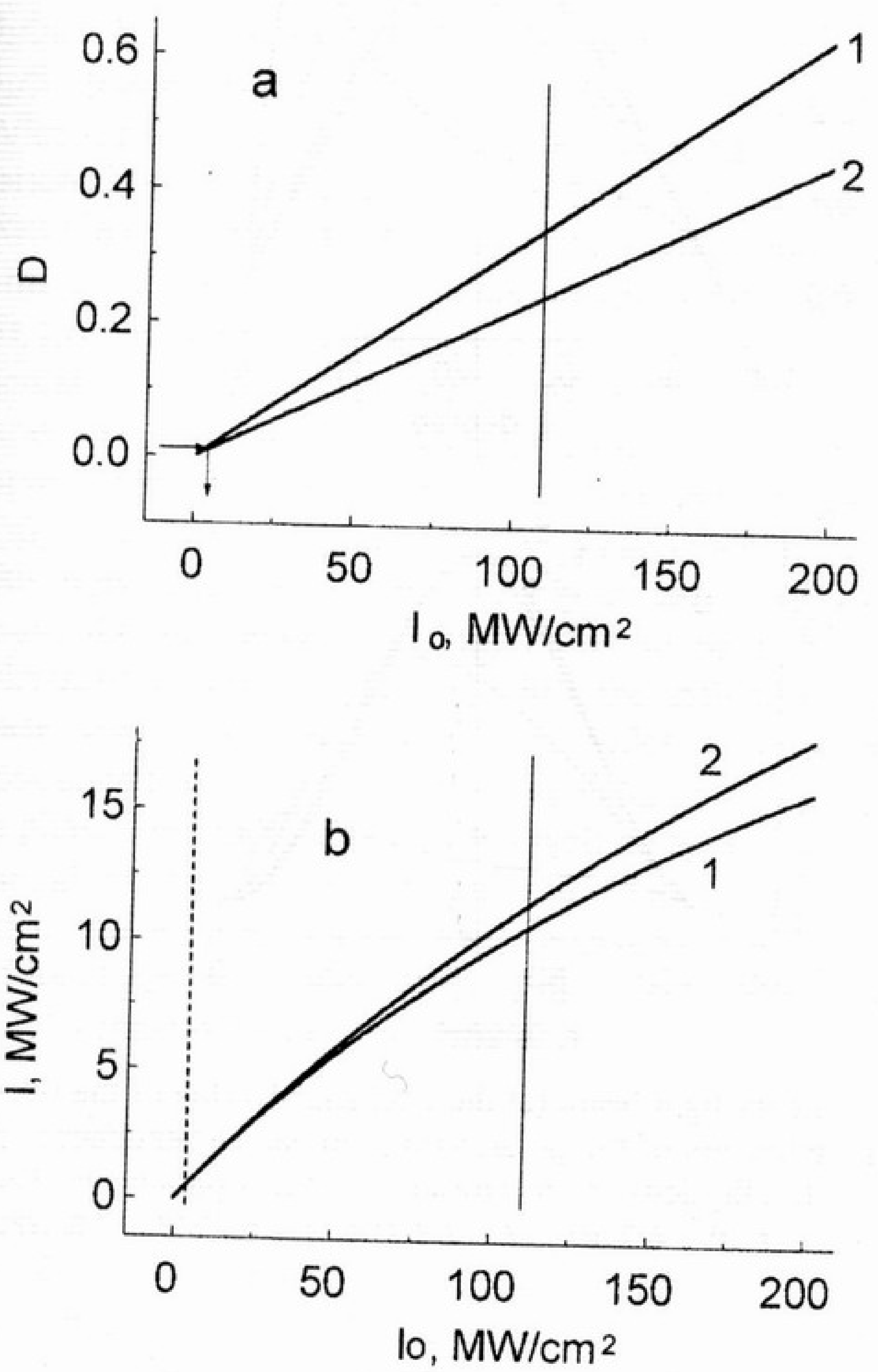

Fig. 11. Dependence on the pumping intensity I_0: a) the second term ($D_\perp$, $D_\parallel$) in the denominator of the formulae (4), (5), b) intensities of light beam ($I_\perp$, $I_\parallel$). The pumping intensity shown by arrow corresponds to $D = 0.01$. The lower limit of the range for changing the pumping intensity is shown by the dotted line, the upper limit of the pumping intensity is shown by the solid line. *1* – $D_\perp$, $I_\perp$; *2* – $D_\parallel$, $I_\parallel$.

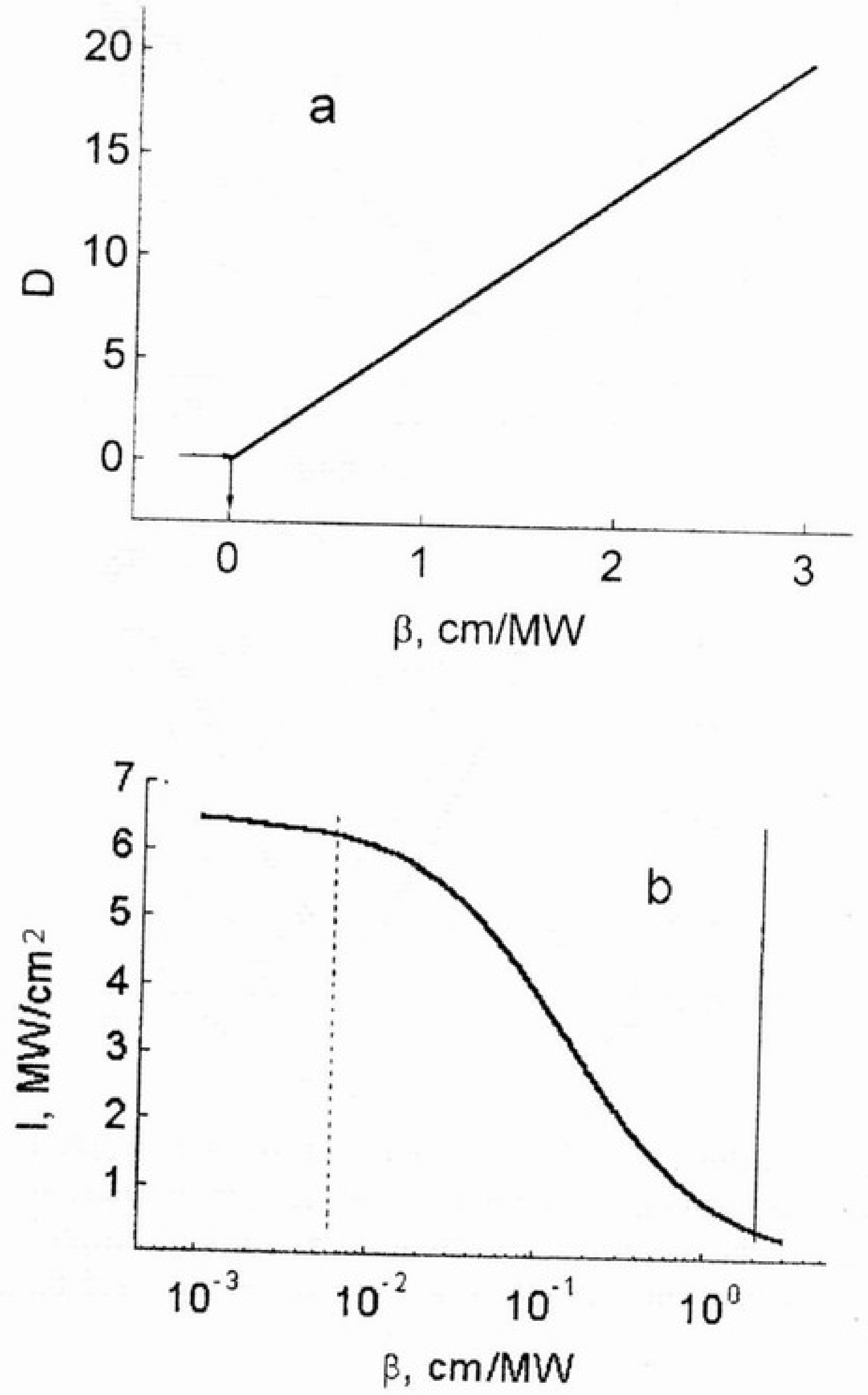

Fig. 12. Dependence on the two-photon absorption coefficient $\beta = \beta_\perp$: a) the second term ($D_\perp$) in the denominator of the formula (4); b) intensity of light beam ($I_\perp$). Dependences of $D_\parallel$ and $I_\parallel$ on $\beta = \beta_\parallel$ coincide with the data of Fig. 12. The value of the two-photon absorption coefficient is shown by arrow, which corresponds to $D = 0.01$. The lower limit of the range for changing the two-photon absorption coefficient is shown by the dotted line, the upper limit of the two-photon absorption coefficient is shown by the solid line. *1* – $D_\perp$, $I_\perp$; *2* – $D_\parallel$, $I_\parallel$.

$\Delta\lambda = \Delta\lambda_g$ it is equal to zero, and for the change of polarization responsible are only intensities of usual and unusual light beams in uniaxial crystal.

Two-photon absorption coefficient. As shown by the formulae (4), (5), it is possible to expect a linear increase in $D_\perp$, $D_\parallel$ values (Fig. 12a), and it is possible to expect a nonlinear decrease in $I_\perp$, $I_\parallel$ (Fig. 12b), when the coefficient of two-photon absorption increases. In accordance with the data of Fig. 12a, the equality of D to 1 % corresponds to $\beta = 6\cdot10^{-3}$ cm/MW. This β value is necessary to be accepted for the lower limit of the range for changing β. As an upper limit, it is possible to take β = (2-3) cm/MW as far as $I_\perp$ and $I_\parallel$ tend to zero, if β exceeds (2-3) cm/MW.

Then the more $\beta_\perp$ differs from $\beta_\parallel$, the greater difference between $I_\perp$ and $I_\parallel$ and the stronger changes the polarization ellipse parameters (Fig. 13). Increasing $\beta_\perp$ at unchanging $\beta_\parallel$ leads to lag of the angle of rotation of the major semiaxis of polarization ellipse (Fig. 13a). Under the gradual increase of $\beta_\perp$ when $\beta_\parallel$ is unchanged, this lag achieves the maximal value that depends on the difference between $\beta_\perp$ and $\beta_\parallel$. At the further increase of φ, lag decreases and tends to zero. Under the gradual increase of $\beta_\perp$ at unchanged $\beta_\parallel$, the ratio of minor semiaxis to the large one (Fig. 13b), eccentricity (Fig. 13c) and focal parameter (Fig. 13d) are changed. If $\beta_\parallel \leq 1\cdot10^{-3}$ cm/MW, it is possible to ignore the influence of two-photon absorption for the extraordinary light beam on parameters of the polarization ellipse. In this case, the intensity of the ordinary light beam and interferential term (third term in the right part of equation (6)) preset shape of curves in Fig. 13.

As the light quantum energy ($h\nu$) increases and tends to the forbidden gap (E_g) of CdS, both $\beta_\perp$ and $\beta_\parallel$ increase [2]. However, the ratio $\beta_\perp/\beta_\parallel$ changes little. It takes place within the range $1.2 < \beta_\perp/\beta_\parallel < 1.7$ [2].

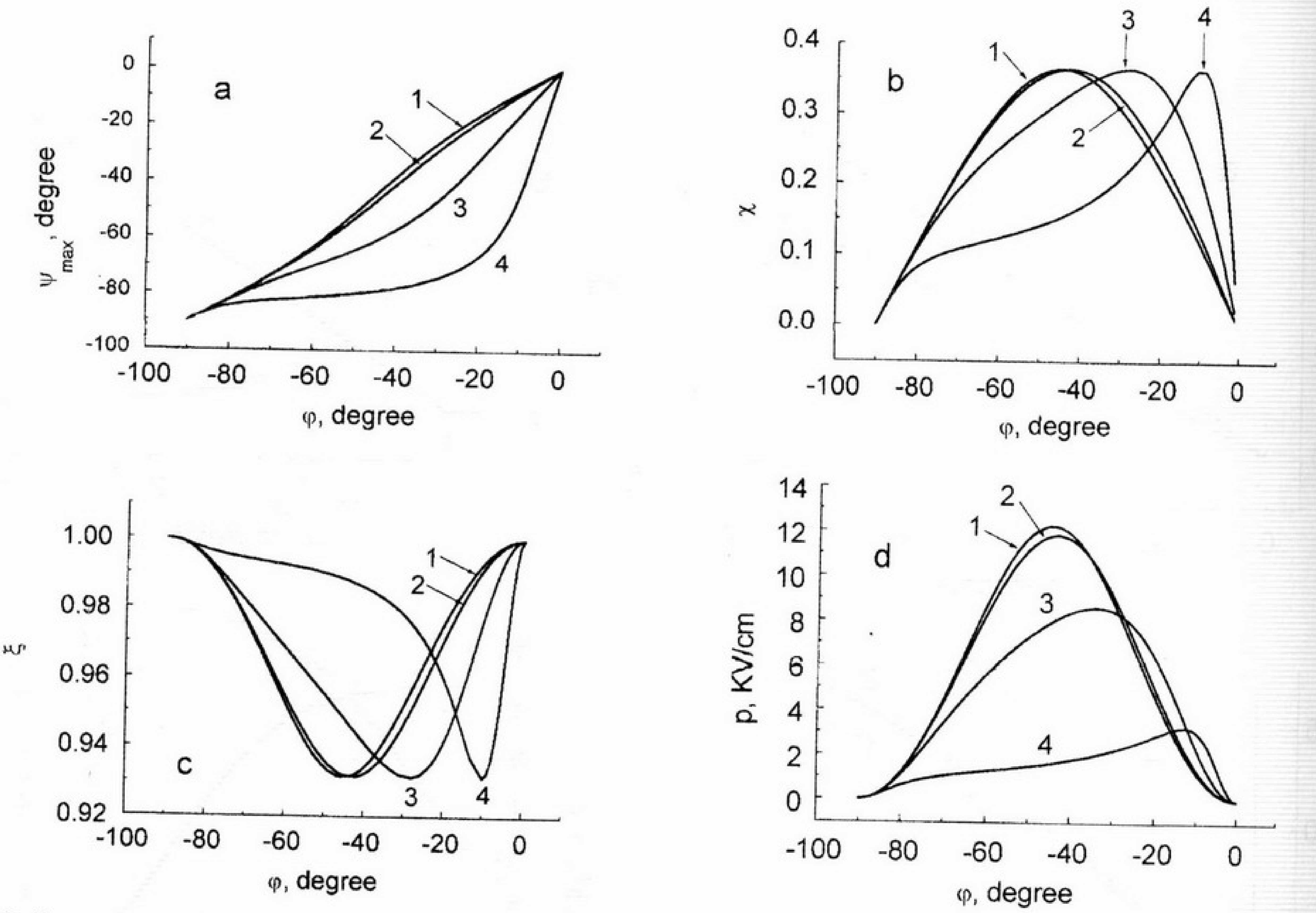

Fig. 13. Influence of the two-photon absorption coefficient $\beta_\perp$ for the ordinary light beam (at the unchanged value of the two-photon absorption coefficient $\beta_\parallel$ for the extraordinary light beam) on parameters of the polarization ellipse. Dependences on the polarization azimuth: a) angle of rotation of ellipse major semiaxis, b) ellipticity, c) eccentricity, d) focal parameter. The values of two-photon absorption coefficients $\beta_\perp$ and $\beta_\parallel$ in cm/MW: *1* – $2.4\cdot10^{-3}$, $1.7\cdot10^{-3}$; *2* – $2.4\cdot10^{-2}$, $1.7\cdot10^{-3}$; *3* – $2.4\cdot10^{-1}$, $1.7\cdot10^{-3}$; *4* – 2.4, $1.7\cdot10^{-3}$.

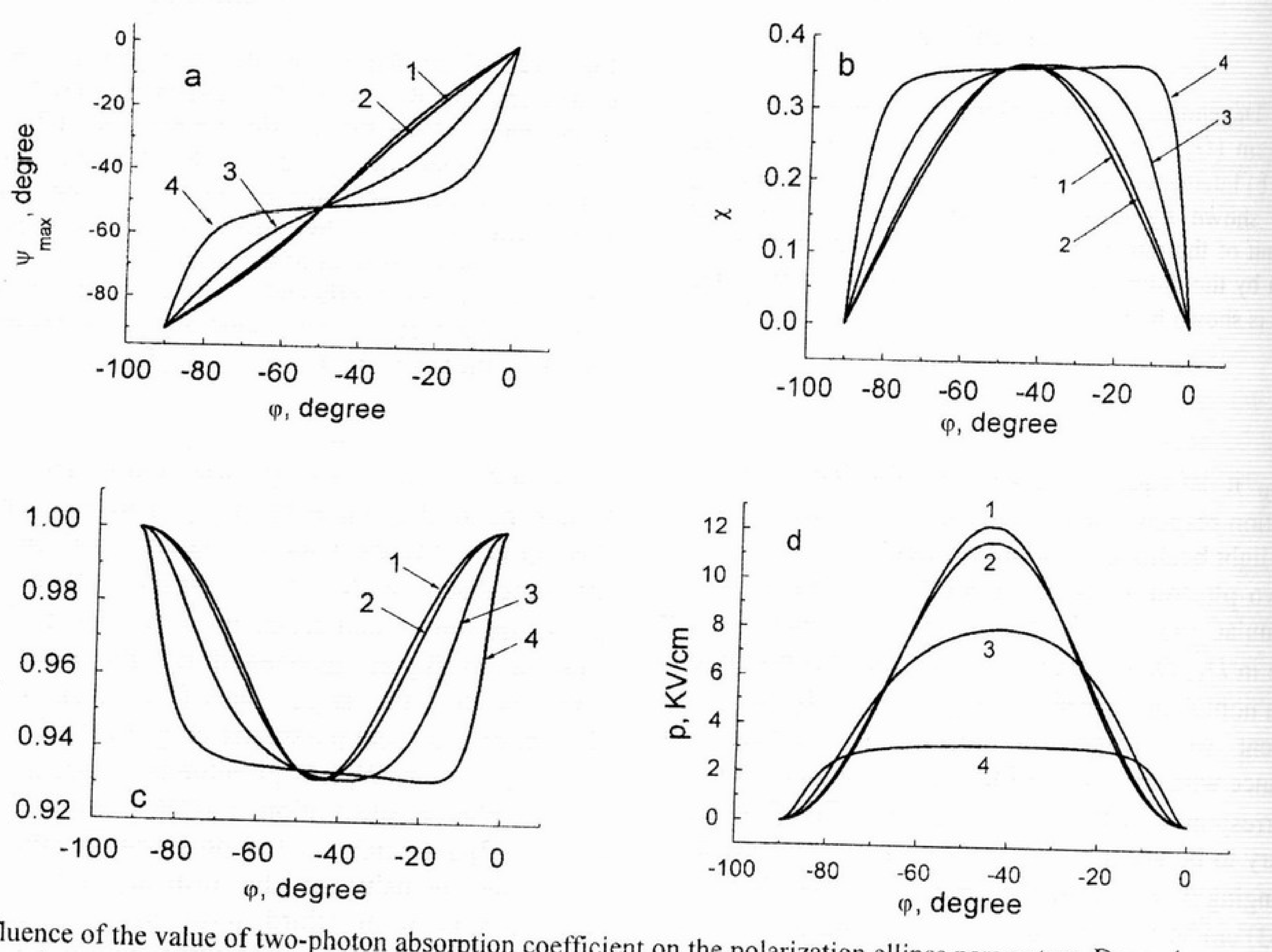

Fig. 14. Influence of the value of two-photon absorption coefficient on the polarization ellipse parameters. Dependences on the polarization azimuth: a) angle of rotation of ellipse major semiaxis, b) ellipticity, c) eccentricity, d) focal parameter. The value of two-photon absorption coefficients $\beta_\perp$ and $\beta_\parallel$ in cm/MW: *1* – $2.4\cdot10^{-3}$, $1.7\cdot10^{-3}$; *2* – $2.4\cdot10^{-2}$, $1.7\cdot10^{-2}$; *3* – $2.4\cdot10^{-1}$, $1.7\cdot10^{-1}$; *4* – 2.4, 1.7.

It is found [2] that for CdS at $\lambda = 694.3$ nm $\beta_\perp/\beta_{||} = 1.4$. It is possible that in other uniaxial crystals $\beta_\perp/\beta_{||}$ possesses another value, therefore, we study the influence of the $\beta_\perp/\beta_{||}$ value on polarization ellipse parameters. We carry out these researches on the example of CdS. Until it is possible to ignore the second term (i.e. $D_\perp$ and $D_{||}$) in the denominator of the formulae (4), (5) (for CdS, approximately to $6\cdot10^{-3}$ cm/MW), the increase in $\beta_\perp/\beta_{||}$ almost does not influence on parameters of the polarization ellipse (compare the curve 1 with the curve 2 in Fig. 14). Further increase in $\beta_\perp/\beta_{||}$ gives rise to $D_\perp$ and $D_{||}$. These become comparable with unity, and then it considerably exceeds unity. As a result, the influence of azimuth on the parameters of polarization ellipse decreases, while the influence of the phase lag angle increases. It provides more clearly pronounced modulation of the dependence $\psi = f(\varphi)$ by the phase lag angle (Fig. 14a) as well as appearance and gradual expansion of the range for values φ, during which the ellipticity (Fig. 14b), eccentricity (Fig. 14c) and focal parameter (Fig. 14d) of the polarization ellipse do not almost depend on the azimuth.

6. Conclusions

Analytical relationships that describe the influence of two-photon absorption on the state of light polarization in uniaxial crystals are obtained. It has been shown that they quantitatively describe the experimentally determined changes of polarization ellipse parameters for light traveling in CdS. It is shown, how one should choose the parameters of crystal and laser to optimize study of the influence of two-photon absorption on light polarization.

It has been found that two-photon absorption a most strongly influences on light polarization, when it is possible to ignore contribution to the light intensity of the interferential term in the formula (5). It can be achieved by either keeping δ at the level 90° or using the light sources with a large width of radiation wave band.

The magnitude of $\Delta\delta_u$ uncertainty forces to keep δ at a specified level, which determines the parameters of crystal and light source. For example, in CdS for $\lambda = 694.3$ nm the uncertainty of $\Delta\delta_\upsilon = \pm1°$ corresponds to the uncertainties in the wavelength $\Delta\lambda_u = \pm0.13$ pm, crystal thickness $\Delta d_u = \pm190$ pm, differences of refraction indexes for ordinary and extraordinary beams $\Delta n_u = \pm7\cdot10^{-9}$. It means that the wavelength of a laser needs to be supported at a set level with the uncertainty $\Delta\lambda_g < \Delta\lambda_u$, and the half-width of laser radiation must be of the order of magnitude equal to $2\Delta\lambda_u$. In the range 20 °C $< t <$ 80 °C, changes in the wavelength by $\Delta\lambda_g = 2\Delta\lambda_u = 0.26$ nm provoke the change of ruby rod temperature the $\Delta t_u = 0.04$ °C. Therefore, the temperature of ruby rod is necessary to be kept with an error less than 0.04 °C. The value of uncertainty in λ bounds the lower limit for the laser pulse duration, since $\tau = 0.5\lambda^2/\Delta\lambda_g c \approx 20$ ns [15].

In CdS, the change of phase lag angle from zero to 180° corresponds to the spectral interval $\Delta\lambda = 24$ pm. If a half-width radiation exceeds this interval by more than two orders, from automatic averaging of the phase lag angle, contribution to the intensity of interferential term in the equation (5) is close to zero. It means that, to study the influence of two-photon absorption on light polarization, it is necessary to use lasers with a pulse width less than 300 fs. The high threshold of optical erosion of semiconductors is advantage of these light sources.

The abovementioned features of two-photon absorption influence on light polarization need to be taken into account when developing highly-efficient generators of the second harmonic [21]; transducers of the pulse width into current [22]; polarization modulators and demodulators of light used for information transfer by pulses of femtosecond duration [23].

References

1. M. Born, E. Wolf, *Principles of Optics*. Pergamon Press, London-New York, 1968.
2. M.S. Brodin, D.B. Goer, Z.A. Demidenko et al., Two-photon absorption in mixed A^2B^6 semiconductor crystals // *Kvantovaya Elektronika* (Kiev) No. 10, p. 56-81 (1976) (in Russian).
3. R.A. Baltrameunas, V.I. Gavryushin, Yu.Yu. Vaitkus, Influence of impurities on two-photon absorption in CdS single crystals // *Fizika tekhnika poluprovodnikov* **18**(4), p. 1150-1153 (1976) (in Russian).
4. M.E. de Souza, Cid B. de Araujo, Two-photon absorption in hexagonal CdS // *Solid State Communs* **48** (11), p. 967-970 (1983).
5. E.V. Beregulin, D.P. Dvornikov, E.L. Ivchenko, I.D. Yaroshevski, Polarization properties and linearly circular dichroism for nonlinear light absorption in A^2B^6 semiconductors // *Fizika tekhnika poluprovodnikov* **9**(5), p. 876-885 (1975) (in Russian).
6. D.P. Dvornikov, E.L. Ivchenko, I.D. Yaroshevski, Linearly circular dichroism in A^3B^5 crystals near the edge of two-photon absorption // *Fizika tekhnika poluprovodnikov* **12**(8), p. 1571-1576 (1978) (in Russian).
7. V.A. Korneichuk, M.P. Lisitsa, I.V. Fekeshgasi, Influence of laser irradiation polarization type on two-photon light absorption in A^2B^6 semiconductors // *Fizika tekhnika poluprovodnikov* **11**(6), p. 192-195 (1977) (in Russian).
8. F. Kaczmarek, *Introduction to Physics of Lasers*. Mir, Moscow, 1981 (in Russian).
9. V.I. Gavrilenko, A.M. Grekhov, D.V. Korbutiak, V.G. Litovchenko, *Optical Properties of*

Semiconductors. Naukova dumka, Kiev, 1987 (in Russian).

10. M. Hercher, Single-mode operation of a Q-switched ruby laser // *Appl. Phys. Lett.* **7** (2), p. 39-41 (1965).
11. S.P. Anokhov, T.Ya. Marusii, M.S. Soskin, *Tuned Lasers*. Radio i svyaz' Publ., Moscow, 1982 (in Russian).
12. E.M. Voronkova, B.N. Grechushnikov, G.I. Distler, I.P. Petrov, *Optical Materials for Infra-Red Technics*. Nauka, Moscow, 1965 (in Russian).
13. N.I. Vitrikhovskii, L.F. Gudymenko, A.F. Maznichenko, Temperature dependence of the refraction index in CdS single crystals // *Fizika tekhnika poluprovodnikov* **2** (6), p. 882-884 (1968) (in Russian).
14. B. Lengyel, *Lasers*. Mir, Moscow, 1964 (in Russian).
15. U.V. Belostotskii, V.M. Lubavskii, V.M. Ovchinnikov, *Principles of Laser Technique*. Sov. radio Publ., Moscow, 1972 (in Russian).
16. Temperature measurement and control catalog / LakeShore Cryotronics, Inc. // *www.lakeshore.com*.
17. Yu.V. Akhsinov, N.V. Morachevskii, V.V. Morozov, F.S. Faizullov, Energy balance and dynamics of damage in dielectrics under laser irradiation // *Fizika tekhnika poluprovodnikov* **14** (6), p. 1756-1760 (1972) (in Russian).
18. A.V. Butenin, B.Ya. Kogan, On the mechanism of optical breakdown in dielectrics // *Kvantovaya elektronika* **5**, p. 143-144 (1971) (in Russian).
19. V.V. Arseniev, Ya.T. Vasiliev, V.S. Dneprovskii, V.U. Khattatov, Destruction of CdS by picosecond light pulses // *Fizika tekhnika poluprovodnikov* **5** (3), p. 403-405 (1971) (in Russian).
20. J. Hermann, B. Wilhelmi, *Ultrashort Optical Pulse Lasers*. Mir, Moscow, 1986 (in Russian).
21. V.G. Dmitriev, V.A. Konovalov, Influence of two-photon absorption of irradiation on the second garmonic generation in crystals // *Kvantovaya elektronika* **6** (3), p. 500-504 (1979) (in Russian).
22. Z. Zheng, A.M. Weiner, J.H. Marsh, M.M. Karkhanehchi, Ultrafast optical thresholding based on two-photon absorption GaAs waveguide photodetectors // *IEEE Photonics Technology Lett.* **9**, p. 493 (1997).
23. H. Ju, S. Zhang. H. De Waardt, Giok-Djan Khoe, H.J.S. Dorren, Ultrafast all-optical switching induced by nonlinear polarization rotation in a multiquantum well semiconductor optical amplifier // *Proc. Symposium IEEE/LEOS Benelux Chapter*, November 20-21, 2003.